Antibiotics

DOI: 10.1002/anie.201003582

NMR Structures of Thiostrepton Derivatives for Characterization of the Ribosomal Binding Site**

Hendrik R. A. Jonker, Sascha Baumann, Antje Wolf, Sebastian Schoof, Fabian Hiller, Kathrin W. Schulte, Karl N. Kirschner, Harald Schwalbe, and Hans-Dieter Arndt**

Dedicated to Professor Peter B. Dervan

Thiopeptides[1] such as thiostrepton (**1**) are highly modified macrocyclic natural products that originate from ribosomal peptide biosynthesis.[2] Compound **1** was identified early[3] as a very potent antibiotic against Gram-positive bacterial pathogens (Scheme 1).[1,4] The X-ray crystal structure of **1** revealed a globular shape reminiscent of folded protein domains.[5] Thiostrepton prominently inhibits protein biosynthesis by binding tightly to the GTPase-associated region (GAR) on the 70S ribosome between the ribosomal protein L11 and the H43/H44 section of the 23S rRNA.[6] Recently, parallel inhibition of the 20S proteasome by **1** was established, thus explaining many of its activities in eukaryotic cells.[7]

In contrast to many other ribosome-targeting antibiotics[8] and despite their exceptional activity in vitro, thiopeptides remain unused in human therapy, mainly because of their very low solubility.[4] A major difficulty in identifying new candidates with improved pharmacokinetics is insufficient data on the key interactions with the adaptive ribosomal RNA and the protein L11. The X-ray structure data for **1** have been used to deduce the binding of **1** to the dynamic L11–rRNA complex by NMR spectroscopy.[6a,9,10] An X-ray structure of single crystals of the intact 50S subunit of the ribosome from *D. radiodurans* soaked with **1** was refined to 3–4 Å resolution.[6b] Biochemical data provide a coherent picture of the overall interaction,[1,6c–e] but as a consequence of the considerable size of **1** and the dynamics of the ribosomal target region, our molecular understanding[6d,e] remained immature. To facilitate the optimization of future compounds we studied the influence of selected molecular changes on the conformational space of thiostrepton (**1**) by using NMR spectroscopy. While **1** and related thiopeptides have been structurally characterized by NMR spectroscopy,[11] investigations on the conformation with current methods are scarce.[12] Here, we report solution-phase structures of **1** and three derivatives, and correlate their molecular interactions at the GAR of the 70S ribosome with their bioactivity.

As a representative member of the thiopeptide family, we modified thiostrepton (**1**) by semisynthesis (Scheme 1). Base-mediated truncation of the residue Dha-17 led to derivative **2**,[6d] and oxidation of ring C at Dcy-9 gave the chemically stable thiazole **3**.[7b] Thiostrepton is configurationally labile,[13] which allowed access to the formally L-cystein-derived epimer **4**. Furthermore, reduction of the dihydropiperidine (Mh6-14) imine function was clean and gave stereoselectively the equatorially substituted piperidine **5**, which closely

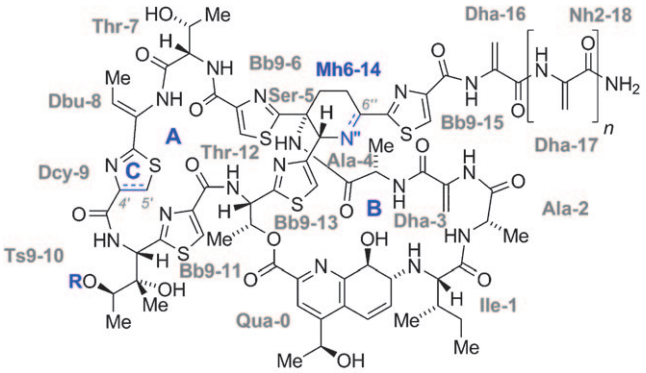

Scheme 1. Molecular structures of **1**–**4** and synthesis of derivatives **5** and **6**. The residues are named in line with literature precedent,[11] the numbering was adapted to biosynthesis.[2] a) $NaBH_3CN$, MeOH; b) Ac_2O (2.2 equiv), 4-dimethylaminopyridine (0.3 equiv), THF (3 mM), 20 °C, 13 h.

[*] Dr. S. Baumann, Dr. S. Schoof, K. W. Schulte, Dr. H.-D. Arndt
Technische Universität Dortmund, Faculty of Chemistry
Otto-Hahn-Strasse 6, 44221 Dortmund (Germany)
and
Max-Planck-Institut of Molecular Physiology
Otto-Hahn-Strasse 11, 44227 Dortmund (Germany)
Fax: (+49) 231-133-2498
E-mail: hans-dieter.arndt@mpi-dortmund.mpg.de

Dr. H. R. A. Jonker, Dipl.-Biochem. F. Hiller, Prof. Dr. H. Schwalbe
Johann Wolfgang Goethe-Universität
Institute for Organic Chemistry and Chemical Biology
Center for Biomolecular Magnetic Resonance (BMRZ)
Max-von-Laue-Strasse 7, 60438 Frankfurt am Main (Germany)
Fax: (+49) 69-7982-9515
E-mail: schwalbe@nmr.uni-frankfurt.de

M. Sc. A. Wolf, Dr. K. N. Kirschner
Fraunhofer-Institute for Scientific Computing (SCAI)
Departments of Bioinformatics and Simulation Engineering
Schloss Birlinghoven, 53754 Sankt Augustin (Germany)

[**] This work was supported in part by the Fonds der Chemischen Industrie (to H.-D.A. and H.S.), the FhG (to K.N.K.), the CEF Macromolecular Complexes and SFB 579 (both to H.S.), and EUNMR. H.-D.A. gratefully acknowledges a DFG Emmy-Noether young investigator award and thanks Prof. Dr. R. Goody for discussions.

Supporting information for this article is available on the WWW under http://dx.doi.org/10.1002/anie.201003582.

resembles the thiopeptins and Sch18640.[14] Under carefully controlled conditions the secondary OH group of the dihydroxyisoleucine (Ts9-10) residue of **1** could be selectively transformed into esters (→**6**). Collectively, these modifications accessed local changes in the scaffold structure, especially in three segments of the important A ring.

We studied the different thiostrepton scaffolds by NMR spectroscopy. As **1**–**5** are barely soluble in biological buffer (low μM range)[6d] and the binding site is largely hydrophobic, the moderately polar and adaptive[15] solvent mixture $CDCl_3$/$[D_5]$EtOH (5:1) was selected for NMR studies in solution.[16] Homo- and heteronuclear NMR spectra (HSQC, HMBC, TOCSY, NOESY) of thiostrepton (**1**) and its derivatives **2**–**5** (5–10 mM) were recorded at 298 K and 600 MHz for the assignment of the ^1H, ^{13}C, and ^{15}N resonances at natural isotope abundance (see the Supporting Information).

The NMR spectra of **1** and **2** were almost identical, which suggests that truncation of the tail does not influence the structure of the core.[6d] All the other compounds gave characteristic features in the ^1H,^{15}N-HSQC fingerprint spectra (Figure 1, top), thus indicating distinct conformations. Proton–proton distances obtained from ^1H,^1H-NOESY spectra were used for the calculation of the solution structure with CNS 1.1[17a] and ARIA 1.2,[17b] by using adapted protocols (see the Supporting Information). NOE build-up data (t_{mix} = 100–600 ms) were used to correct for spin diffusion,[18] and ^1H,^1H-ROESY was utilized to eliminate data for nuclei prone to undergo chemical exchange.[19] The excellent resolution of the spectra allowed a large number of NOE distance restraints to be obtained for all samples (Table 1). These comprehensive data resulted in compact structure bundles (Figure 1, bottom). As a consequence of the many well-defined NOE signals and the ARIA algorithm, these tightly converged ensembles probably underrate the true flexibility of the molecules, but represent the average minimum-energy solutions very well.

Table 1: Key structure determination and docking score data.

Sample	NOEs[a]	RMSD[b,c]	X-ray[b,d]	Score[e]	Score[f]
1	231 (38)	0.43/0.42/0.42	0.77	−8.41/4	−8.35/14
3	167 (8)	0.43/0.42/0.43	1.09	−8.54/23	−8.54/23
4	170 (13)	0.43/0.43/0.44	1.83	−8.30/6	−7.92/34
5	220 (29)	0.45/0.42/0.44	1.02	−9.15/2	−8.71/20

[a] Total number of NOE-based distance restraints, ambiguous NOE connections in parentheses. [b] Root mean square deviation in Å. [c] Bundle/A ring only/B ring only. [d] Average RMSD in Å for the heavy atoms in the A ring region (residues 6–11) compared to the X-ray structure aligned on the identical B ring. [e] Best AUTODOCK docking score/number of conformations. [f] Largest cluster docking score/number of conformations.

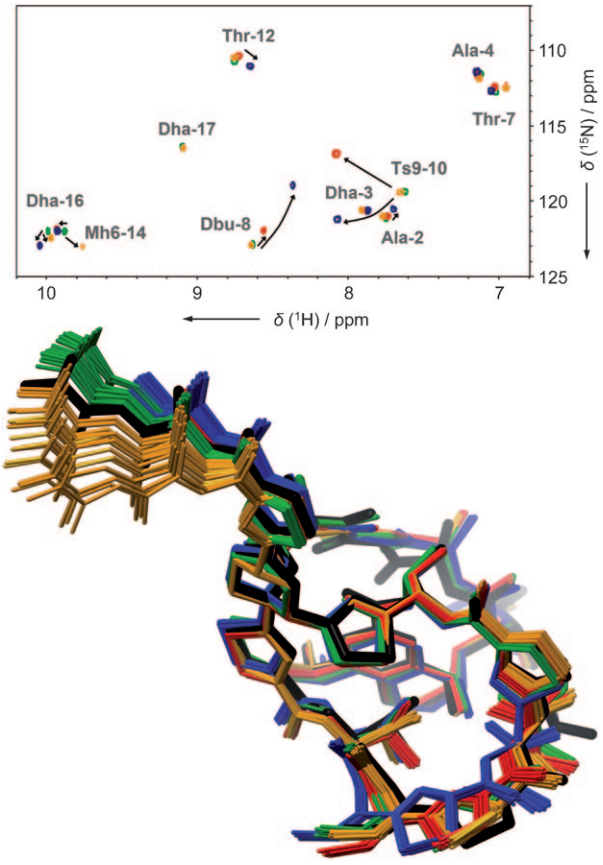

Figure 1. Top: Assigned overlay of ^1H,^{15}N-HSQC spectra for **1** (green), **3** (red), **4** (blue), and **5** (orange) at natural isotope abundance. Bottom: Bundle of 20 minimum-energy NMR solution structures of compounds **1** (PDB code 2L2W), **3** (2L2X), **4** (2L2Y), and **5** (2L2Z) superimposed on the previously known X-ray crystal structure of thiostrepton (black, 1E9W).

The solution structure of thiostrepton (**1**) determined by NMR spectroscopy compares very well with the X-ray crystal structure (PDB 1E9W),[5] thus validating our approach. The structure of the quinaldic acid macrocyle (ring B) and the dehydrolanine tail are nearly identical for all derivatives. The dehydroalanine tails of **3** and **4** could not be fully compared, but the remaining parts were very similar. The main structural differences occur in the conformation of the thiazoline-bearing A ring, specifically in residues 7–10. Their orientation significantly deviates in the oxidized compound **3** and, in particular, the epimer derivative **4** (Figure 1, bottom). The C ring (Dcy, Cys, Bb9) and the dihydroxyisoleucine side chain (Ts9-10) become displaced by 2.5–2.9 Å.

Oxidation of the C ring flattens this subunit, but causes only a slight displacement of the adjacent dihydroxyisoleucine residue. Consistently, we observe perturbation of the chemical shift of the amide of residue 10. The alteration in stereochemistry in epimer **4** leads to a much larger change in the structure, with a significant dislocation of ring C as indicated by the large change in the amide chemical shift of the proximal Dbu-8 and Ts9-10 residues. Moreover, the adjacent thiazole ring (Ts9-10, Bb9-11) becomes tilted by 22°. A change in its environment is reflected by the chemical shift perturbations of the amide groups of the residues Ts9-10 and Thr-12. For compound **5**, similar changes are observed for the piperidine (residues 5 and 14) and the adjacent thiazole ring (residue 15), thus confirming that the structure of the core is not strongly affected, but the orientation of the dehydroalanine tail is.

Deuterium exchange kinetics along with the temperature dependence of the chemical shifts for amide groups in **1** indicated that the internal hydrogen bonds of the Ser-5, Thr-7, and Ts9-10 backbone amides[5] are likely preserved in solution (see the Supporting information). These residues are in proximity to the nitrogen atoms of the adjacent thiazol(in)e ring, which could explain their high protection against exchange. In line with earlier reports,[12] we found atypical properties for the dehydroamino acids, which likely reflects their enamine character.

The structure of the dehydroalanine tail region could not be well defined by NMR spectroscopy. Therefore, its flexibility was assessed by gas-phase quantum-mechanical calculations (HF/6-31G*) of torsion potentials for a truncated analogue (see the Supporting Information).[20] Seven minima were found over 360° rotations, all within 5 kcal mol^{-1} of each other. The barriers for interconversion were on the order of 7–8 kcal mol^{-1}, which indicates that the tails are fairly flexible. Gas-phase calculations rarely underestimate energies in the condensed phase, because stabilizing solvent or binding partners are absent. The tail can hence be safely assumed to sample an extended volume in solution[6c] and to undergo conformational adaptation on binding.[6b]

Docking studies were then performed with AUTODOCK.[21] NMR structure ensembles generally cover a significant area of the energetically accessible conformational space, even though they may underestimate the truly accessible fluctuations.[22] We therefore docked all the individual members from the NMR-derived structure ensembles for **1**, its oxidized (**3**), epimer (**4**), and its reduced variant (**5**) onto the large ribosomal subunit in its thiostrepton-bound state (PDB 3CF5).[23] The crystal-structure coordinates of the L11 protein and 23S RNA were used to define the structure of the binding site. By using these data for the completely rigid docking of **1**, we consistently found poses where the dehydroalanine tail was inserted deeply into the cleft formed by L11 and 23S. Neither the recent structural data nor our PICC studies, which localized the Dha tail biochemically, support such a binding geometry.[6]

In a more refined semirelaxed docking approach, the side chains of the ligand and the tail residues were treated as flexible.[24] For all four structures, we identified poses with the best docking scores that resemble the overall binding mode in the crystal structure (Figure 2, top). These findings indicate that the flexibility of the side chains and the tail residues is important for proper binding to the target structure. Interestingly, much less consistent docking results were obtained when we implemented a scoring function developed for RNA targets.[25] These data suggest that despite the binding environment being dominated by RNA,[6e] the binding site characteristics are more similar to a typical nonpolar protein receptor than to isolated RNA. In fact, only surface-oriented base–ligand contacts and no charge–charge interactions are present.

A statistical evaluation of the binding conformations (Figure 2, bottom) consistently identified the crystal-like binding mode for **1**, **3**, and **5**, which exhibited comparable interactions with the binding site (see the Supporting Information). In this analysis, the side-chain OH groups of

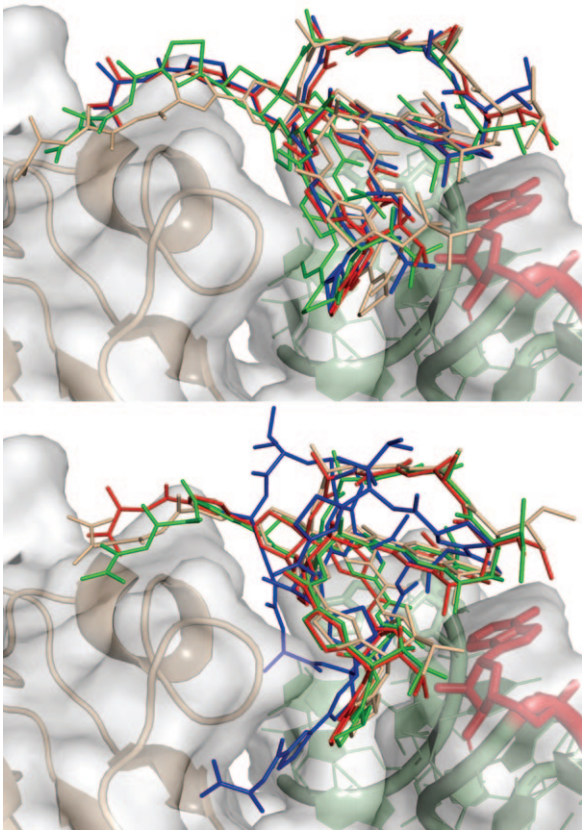

Figure 2. Docking of **1** (green), **3** (red), **4** (blue), and **5** (light orange) to the L11 protein (gray, only a backbone trace is shown) and 23S rRNA (dark green). The van der Waals surface is shaded gray, the crucial nucleobase A1067 is highlighted (red). Top: Poses with the best docking scores. Bottom: Representative poses from the largest clusters. Note the reverted binding pose being highly populated for **4**.

Thr-7 and Ts9-10 form three hydrogen bonds to A1067, and Bb9-6 displays a stacking interaction with A1095. The tail of **3** and **5** forms an additional hydrogen bond to the protein backbone. In contrast, most of these characteristic binding features were absent for epimer **4**. Furthermore, the unlikely[6c] tail-in-cleft binding mode was frequently found. Taken together, these data and the lower score of the biochemically supported "best" solution strongly suggest that the epimer **4** is less well suited for binding to the target structure.

The docking studies ranked the reduced form **5** as the tightest binder, and placed thiostrepton (**1**) and the oxidized form **3** with nearly equal affinity in between **5** and **4** (Table 1). This computational trend was confirmed by biochemical measurements.[23] Ligand affinities to the target were determined by using a fluorescence-polarization-based assay.[6d,e] A coupled in vitro transcription-translation assay was implemented to assess the functional inhibition constants for bacterial protein synthesis. We used a GFP reporter gene construct to generate mRNA in situ with T7 polymerase, which was directly translated into detectable green fluorescent protein (GFP) by using *E. coli* cell lysate.[26] The temperature and timing of the coupled reactions were optimized to ensure a stable readout (see the Supporting Information).

Thiostrepton (**1**), its truncated variant **2**, and the oxidized form **3** show very similar activity. A significantly reduced affinity to the target (20–25 fold) was found for epimer **4**, which was also evident in much smaller inhibition zones on agar plates (see the Supporting Information). Surprisingly, **4** displayed an IC_{50} value similar to **1** in the translation inhibition assay, but HPLC tracking experiments confirmed that the more stable D epimer[13] was reformed from **4** over a period of several hours in the presence of translationally competent cell lysate. As predicted by docking studies, **5** had a significantly increased affinity to the isolated target—comparable to the highly active nosiheptide.[1,6d] The monocyclic thiopeptides micrococcin and thiotipin had a 10–1000-fold (thiotipin) reduced affinity for the isolated target, and translation inhibition in line with the binding data.[27,28] Interestingly, cleaving the B ring of thiostrepton to give a single macrocycle[13] led to an even less potent compound (**7**). These findings indicate that monomacrocyclic micrococcin might be special in targeting a binding mode different from **1**.[6b,e,29]

Within the whole class of thiopeptides, the dihydroxyisoleucine (Ts9-10) residue is unique to thiostrepton (**1**).[1] The docking analysis suggested that Ts9-10 forms hydrogen bonds with the ribose of A1067. Compound **6**, which features an acylated secondary OH group on this residue displayed a tenfold reduced affinity to the target, and a twofold reduced efficacy in translation inhibition. This result indicates that the side-chain OH groups of Ts9-10 enhance the efficacy of **1**, very likely because of their hydrogen-bonding capacity.

The L-cystein epimer **4** showed a narrowing of the cleft between the A and B rings, which leads to a shape mismatch with the target structure. The insertion of the dehydrobutyrine residue (Dbu-8) between the RNA and the L11 protein as well as the placement of Ts9-10 at the A1067 residue then suffers. It is remarkable how well the experimental data was qualitatively captured by the integrated NMR-docking procedure (Table 2), particularly given the moderate resolution of the target X-ray structure (3–4 Å). This trend strongly suggests that the inhibitor structures do not undergo major conformational reorganization on binding to the target. Thiopeptide inhibitors may have evolved to mimic this recognition motif, for example, to mimic domain V of the elongation factor EF-G in one of the states during the PRE to POST transition of the ribosome.[30,31]

In summary, integrated semisynthesis, NMR spectroscopic solution-structure determination, computation, and biological evaluation studies have identified key conformational and structural parameters involved in thiostrepton targeting the ribosome's GAR.[23] This ternary ligand–RNA–protein interaction seems to be driven by ligand shape and RNA recognition,[6e] but is moderately tolerant of structure variation. The NMR analysis of the structures of thiostrepton (**1**) and the derivatives **2**–**5** revealed that the molecular scaffold of **1** may not be perfect for addressing the pharmacophore region of this highly complex RNA–protein target. The minor mismatch seems to be healed in part by the dihydroxyisoleucine side chain. Overall, these data define structural boundaries, wherein an improvement of the overall pharmacological profile of these compounds or their analogues will be possible.

Table 2: Determination of the biological activity.

Compound	K_D(L11/RNA) [nM][a]	IC_{50} [μM][b]
1 (TS)	0.26 ± 0.06	0.69 ± 0.03
2 (TS-1)	0.25 ± 0.06	0.80 ± 0.18
3 (ox-TS-1)	0.30 ± 0.14	0.88 ± 0.06
4 (epi-TS-1)	7.4 ± 1.4	(0.63 ± 0.08)[c]
5 (red-TS)	0.14 ± 0.07	–
nosiheptide	0.14 ± 0.08	–[d]
micrococcin	2.3 ± 1.2	1.69 ± 0.12
thiotipin	240 ± 13	7.02 ± 1
7 (B-ring cleaved)	882 ± 69	8.01 ± 2.8
6 (Ac-TS)	2.4 ± 0.28	1.67 ± 0.42

[a] Apparent affinity to the reconstituted minimal L11–rRNA target complex (*T. thermophilus*. [b] IC_{50} for the coupled transcription-translation reporter assay in vitro. [c] Re-equilibrates to **2** during the experiment (see text). [d] Complicated by ligand autofluorescence. See the Supporting Information for details.

Received: June 11, 2010
Revised: September 20, 2010
Published online: March 1, 2011

Keywords: antibiotics · drug design · NMR spectroscopy · ribosomes · thiopeptides

[1] Reviews: a) M. C. Bagley, J. W. Dale, E. A. Merritt, X. Xiong, *Chem. Rev.* **2005**, *105*, 685–714; b) R. A. Hughes, C. J. Moody, *Angew. Chem.* **2007**, *119*, 8076–8101; *Angew. Chem. Int. Ed.* **2007**, *46*, 7930–7954.

[2] Reviews: a) H.-D. Arndt, S. Schoof, J.-Y. Lu, *Angew. Chem.* **2009**, *121*, 6900–6904; *Angew. Chem. Int. Ed.* **2009**, *48*, 6770–6773; b) C. Li, W. L. Kelly, *Nat. Prod. Rep.* **2010**, *27*, 153–164.

[3] a) J. F. Pagano, M. J. Weinstein, H. A. Stout, R. Donovick, *Antibiot. Ann.* **1955/1956**, 554; b) J. Vandeputte, J. D. Dutcher, *Antibiot. Ann.* **1955/1956**, 560; c) B. A. Steinberg, W. P. Jambor, L. O. Suydam, A. Soriano, *Antibiot. Ann.* **1955/1956**, 562.

[4] a) G. H. Nesbitt, P. R. Fox, *Vet. Med. Small Anim. Clin.* **1981**, *76*, 535–538; b) T. Kieser, M. J. Bibb, M. J. Buttner, K. F. Chater, D. A. Hopwood, *Practical Streptomyces Genetics*, John Innes Foundation, Norwich (UK), **2000**.

[5] a) B. Anderson, D. Crowfoot-Hodgkin, M. A. Viswamitra, *Nature* **1970**, *225*, 233–235; b) C. S. Bond, M. P. Shaw, M. S. Alphey, W. N. Hunter, *Acta Crystallogr. Sect. D* **2001**, *57*, 755–758.

[6] Recent progress: a) H. R. A. Jonker, S. Ilin, S. K. Grimm, J. Wöhnert, H. Schwalbe, *Nucleic Acids Res.* **2007**, *35*, 441–454; b) J. M. Harms, D. N. Wilson, F. Schlünzen, S. R. Connell, T. Stachelhaus, Z. Zaborowska, C. M. T. Spahn, P. Fucini, *Mol. Cell* **2008**, *30*, 26–38; c) S. Baumann, S. Schoof, S. D. Harkal, H.-D. Arndt, *J. Am. Chem. Soc.* **2008**, *130*, 5664–5666; d) S. Schoof, S. Baumann, B. Ellinger, H.-D. Arndt, *ChemBioChem* **2009**, *10*, 242–245; e) S. Baumann, S. Schoof, M. Bolten, C. Haering, M. Takagi, K. Shin-ya, H.-D. Arndt, *J. Am. Chem. Soc.* **2010**, *132*, 6973–6981.

[7] a) U. G. Bhat, M. Halasi, A. L. Gartel, *PLoS ONE* **2009**, *4*, e6593; b) S. Schoof, G. Pradel, M. N. Aminake, B. Ellinger, S. Baumann, M. Potowski, Y. Najajreh, M. Kirschner, H.-D. Arndt, *Angew. Chem.* **2010**, *122*, 3389–3393; *Angew. Chem. Int. Ed.* **2010**, *49*, 3317–3321.

[8] J. Poehlsgaard, S. Douthwaite, *Nat. Rev. Microbiol.* **2005**, *3*, 870–881.

[9] G. Lentzen, R. Klinck, N. Matassova, F. Aboul-ela, A. I. H. Murchie, *Chem. Biol.* **2003**, *10*, 769 – 778.
[10] a) M. A. Markus, A. P. Hinck, S. Huang, D. E. Draper, D. A. Torchia, *Nat. Struct. Biol.* **1997**, *4*, 70 – 77; b) A. P. Hinck, M. A. Markus, S. Huang, S. Grzesiek, I. Kustonovich, D. E. Draper, D. A. Torchia, *J. Mol. Biol.* **1997**, *274*, 101 – 113; c) S. Ilin, A. Hoskin, O. Ohlenschläger, H. R. A. Jonker, H. Schwalbe, J. Wöhnert, *ChemBioChem* **2005**, *6*, 1611 – 1618; d) D. Lee, J. D. Walsh, P. Yu, M. A. Markus, T. Choli-Papadopoulou, C. D. Schwieters, S. Krüger, D. E. Draper, Y. X. Wang, *J. Mol. Biol.* **2007**, *367*, 1007 – 1022.
[11] a) K. Tori, K. Tokura, Y. Yoshimura, Y. Terui, K. Okabe, H. Otsuka, K. Matsuhita, F. Inagaki, T. Miyazawa, *J. Antibiot.* **1981**, *34*, 124 – 129; b) O. D. Hensens, G. Albers-Schönberg, B. F. Anderson, *J. Antibiot.* **1983**, *36*, 799 – 813; c) U. Mocek, J. M. Beale, H. G. Floss, *J. Antibiot.* **1989**, *42*, 1649 – 1652.
[12] a) B.-S. Yun, K.-i. Fujita, K. Furihata, H. Seto, *Tetrahedron* **2001**, *57*, 9683 – 9687; b) R. J. Lewis, R. A. Hughes, L. Alcaraz, S. P. Thompson, C. J. Moody, *Chem. Commun.* **2006**, 4215 – 4217.
[13] S. Schoof, H.-D. Arndt, *Chem. Commun.* **2009**, 7113 – 7115.
[14] a) O. D. Hensens, G. Albers-Schönberg, *J. Antibiot.* **1983**, *36*, 814 – 831; b) M. S. Puar, A. K. Ganguly, A. Afonso, R. Brambilla, P. Mangiaracina, O. Sarre, R. D. MacFarlane, *J. Am. Chem. Soc.* **1981**, *103*, 5231 – 5233.
[15] R. Gratias, H. Kessler, *J. Phys. Chem. B* **1998**, *102*, 2027 – 2031.
[16] We also conducted preliminary structure determinations in [D_6]DMSO, [D_3]TFE, and their aqueous mixtures, all with much inferior results.
[17] a) A. T. Brünger, P. D. Adams, G. M. Clore, W. L. DeLano, P. Gros, R. W. Grosse-Kunstleve, J. S. Jiang, J. Kuszewski, M. Nilges, N. S. Pannu, R. J. Read, L. M. Rice, T. Simonson, G. L. Warren, *Acta Crystallogr. Sect. D* **1998**, *54*, 905 – 921; b) J. P. Linge, S. I. O'Donoghue, M. Nilges, *Methods Enzymol.* **2001**, *339*, 71 – 90.
[18] J. P. Linge, M. Habeck, W. Rieping, M. Nilges, *J. Magn. Reson.* **2004**, *167*, 334 – 342.
[19] A. Bax, S. Grzesiek in *Encyclopedia of Nuclear Magnetic Resonance*, *Vol. 7* (Eds.: E. D. Becker, J. W. Emsley, B. C. Gerstein, S. I. Chan, T. C. Farrar, A. McDermott), Wiley, New York **1996**, pp. 4157 – 4166.
[20] GAMESS (http://www.msg.ameslab.gov/gamess/gamess.html) was used: M. S. Gordon and M. W. Schmidt in *Theory and application of computational chemistry: The first forty years* (Eds.: C. E. Dykstra, G. Frenking, K. S. Kim, G. E. Scuseria), Elsevier, Amsterdam **2005**, pp. 1167 – 1189.
[21] G. M. Morris, D. S. Goodsell, R. S. Halliday, R. Huey, W. E. Hart, R. K. Belew, A. J. Olson, *J. Comput. Chem.* **1998**, *19*, 1639 – 1662.
[22] C. A. E. M. Spronk, S. B. Nabuurs, A. M. J. J. Bonvin, E. Krieger, G. W. Vuister, G. Vriend, *J. Biomol. NMR* **2003**, *25*, 225 – 234.
[23] The experimental conditions are slightly different because of the paucity of structural data (*D. radiodurans*) and reliable binding (*T. thermophilus*) and translation inhibition assays (*E. coli*). However, a high degree of conservation of the GAR structure and function among species justifies the comparison. For details, see D. N. Wilson, K. H. Nierhaus, *Crit. Rev. Biochem. Mol. Biol.* **2005**, *121*, 991 – 1004, and Ref [6].
[24] For a related technique, see B. Stauch, B. Simon, T. Basile, G. Schneider, N. P. Malek, M. Kalesse, T. Carlomagno, *Angew. Chem.* **2010**, *122*, 4026 – 4030; *Angew. Chem. Int. Ed.* **2010**, *49*, 3934 – 3938.
[25] P. Pfeffer, H. Gohlke, *J. Chem. Inf. Model.* **2007**, *47*, 1868 – 1876.
[26] M. B. Iskakova, W. Szaflarski, M. Dreyfus, J. Remme, K. H. Nierhaus, *Nucleic Acids Res.* **2006**, *34*, e135.
[27] We thank Dr. M. Brönstrup (Sanofi-Aventis, Frankfurt, Germany) and Dr. K. Shin-ya (BIRC Tokyo, Japan) for analytical samples of nosiheptide, micrococcin, and thiotipin, respectively.
[28] The high concentration of ribosomes (μM) and the complex coupled assay kinetics allows only a qualitative comparison of translation inhibition and binding data.
[29] A. A. Bowers, M. G. Acker, A. Koglin, C. T. Walsh, *J. Am. Chem. Soc.* **2010**, *132*, 7519 – 7527.
[30] a) M. V. Rodnina, A. Savelsbergh, N. B. Matassova, V. I. Katunin, Y. P. Semenkov, W. Wintermeyer, *Proc. Natl. Acad. Sci. USA* **1999**, *96*, 9586 – 9590; b) H. Stark, M. V. Rodnina, H. J. Wieden, M. van Heel, W. Wintermeyer, *Cell* **2000**, *100*, 301 – 309.
[31] Y.-G. Gao, M. Selmer, C. M. Dunham, A. Weixlbaumer, A. C. Kelley, V. Ramakrishnan, *Science* **2009**, *326*, 694 – 699.

